Kinetic Isotope Effects for Hydrogen Abstraction from Various Saturated Hydrocarbons by Deuterium Atoms in the Gas Phase

Noboru Fujisaki, Tino Gäumann, and Amanz Ruf

Institute of Physical Chemistry, Federal School of Technology, CH-1015 Lausanne, Switzerland

Chemical Kinetics / Gases / Isotope Effects / Radiation Chemistry / Radicals

Using deuterium atoms produced in the radiolysis of heavy water vapor, the kinetic isotope effects k_H/k_D were determined by the isotope competitive method for the abstraction reaction $D^{\bullet} + RH(R'D) \xrightarrow{k_H/k_D} HD(D_2) + R^{\bullet}(R'^{\bullet})$, where RH is an alkane and R'D is the corresponding perdeuterated alkane. The alkanes RH investigated include isobutane, 2,3,4-trimethylpentane, neopentane, cyclopentane, cyclohexane, cycloheptane, and n-heptane. The results were represented in terms of the Arrhenius-type expression $k_H/k_D = A_H/A_D \exp((E_D - E_H)\ (\text{kJ mol}^{-1})/RT)$, over the temperature range 363–473 K. The pre-exponential factor ratios A_H/A_D vary from 0.36 for neopentane to 0.70 for 2,3,4-trimethylpentane, the $E_D - E_H$ values from 6.4 for 2,3,4-trimethylpentane to 10.4 kJ mol^{-1} for neopentane. The variation in the $E_D - E_H$ values was correlated with the bond strength of the C–H bond being broken. The deuterium and hydrogen atoms, as the attacking species, are found to show essentially the same magnitude of the kinetic isotope effects in the hydrogen abstraction from a given alkane. The theoretical calculations of the isotope effects have been carried out on the basis of transition-state theory combined with the London-Eyring-Polanyi-Sato potential energy surface. Good agreement was obtained between experiment and theory, when tunnel effects were taken into consideration.

1. Introduction

Atomic hydrogen is one of the fundamental reactive species, and plays an important part in the vacuum-ultraviolet photolysis [1,2] and radiolysis [3,4] of hydrocarbons as well as in combustion processes [5]. For this reason, the Arrhenius parameters have been determined for the reaction of H-atoms with a large number of substances [6–12]. However, the data are scant for the reaction of H-atoms with deuterated compounds [12].

We have already determined the kinetic isotope effects (KIEs) for the reactions of hydrogen atoms with a dozen hydrocarbons [13–16]. As a further extension, the KIEs for the reactions of deuterium atoms with alkanes have been measured in the present work by making use of the radiolysis of heavy water vapor as the source of deuterium atoms.

Much insight into reaction mechanisms may be gained from the study of the KIE. In fact, in order to understand the KIE we have to invoke terms such as the potential-energy surface of a reacting system, vibrational frequencies of reactants and activated complexes, and tunnel correction factors. The theoretical calculations of the KIEs for the H-atom reactions were successful [14, 15], and now it seems worthwhile to see whether or not the theory is capable of reproducing the experimental KIEs for the D-atom reactions, too.

2. Experimental

Heavy water (>99 atom% D) was obtained from the Federal Institute for Reactor Research (Zürich). It was distilled first from a potassium permanganate solution containing KOD and then without any additive. The paraffines and its isotopic counterparts were rigorously purified to >99.9% by preparative gas chromatography [13–16]. The isotopic purities of the deuterated paraffins were generally better than 99 atom% D [13–16]. The mole fractions of the deuterated hydrocarbon in the nondeuterated and deuterated hydrocarbon mixtures were usually 0.6, 0.7, 0.8, and 0.9. In typical runs, 0.55 g of heavy water and 12 mg of the hydrocarbon mixture were transferred into a Pyrex spherical vessel of 540 ml provided with a break seal after degassing the samples.

The samples were irradiated in a ^{60}Co γ-ray source (Gammacell 220) at a dose rate of 5.2 kGy/h to a total dose of 5.0 kGy. Unless otherwise specified, the samples were irradiated at 363, 393, 423, 453, and 473 K. The isotopic hydrogen formed was collected with a Toepler pump and subsequently analyzed at 77 K by gas chromatography on a column packed with etched glass beads. Further details of the method of irradiation and product analysis have been described elsewhere [13–17].

3. Results

3.1. Reaction Mechanism

Table 1 shows the radiation chemical yield *G* for deuterium molecules produced in the radiolysis of pure heavy water vapor as a function of total dose. To the best of our knowledge, the *G* value for D_2 from γ-radiolysis of pure D_2O vapor has not been reported so far. As will be shown later, the *G* values for D_2 from pure D_2O vapor are negligibly small compared to *G* values for isotopic hydrogen from D_2O vapor with small concentrations of hydrocarbons. The formation of isotopic hydrogen from water vapor has been interpreted on the basis of the following reaction scheme [13–16, 18]:

$$D_2O \rightsquigarrow D_2O^{\bullet +} + e^- \tag{1}$$

$$D_2O \rightsquigarrow D_2O^* \tag{2}$$

$$D_2O^{\bullet +} + D_2O \longrightarrow D_3O^+ + OD^{\bullet} \tag{3}$$

$$D_3O^+ + nD_2O \longrightarrow D^+(D_2O)_{n+1} \tag{4}$$

$$D^+(D_2O)_{n+1} + e^- \longrightarrow D^{\bullet} + (n+1)D_2O \tag{5}$$

$$D_2O^* \longrightarrow D^{\bullet} + OD^{\bullet} \tag{6}$$

$$D_2O^* \longrightarrow D_2 + O \tag{7}$$

Table 1
G value for D_2 produced in the radiolysis of pure heavy water vapor[a)]

Dose (10^{-1} kGy)	1.0	2.0	4.0	8.0
$G(D_2)$[b)]	0.15	0.09	0.01	0.01

[a)] Experimental conditions: $P_{D_2O} = 1.78 \cdot 10^5$ Pa, $V = 0.54$ dm^3, $T_{\text{irradiat.}} = 423$ K.

[b)] The term *G* value stands for the number of molecules formed per 100 eV of energy absorbed by the system.

Ber. Bunsenges. Phys. Chem. 90, 375–382 (1986) – © VCH Verlagsgesellschaft mbH, D-6940 Weinheim, 1986.
0005-9021/86/0404-0375 $ 02.50/0

where D_2 refers to the deuterium molecule eliminated in the unimolecular mechanism. The formation of both the oxygen atom and the unimolecularly detached deuterium is of minor importance here [13–16, 18]. Although the $D^{\bullet}$ and $OD^{\bullet}$ radicals are produced with comparatively large yields, i.e., $G(D^{\bullet}) \approx G(OD^{\bullet}) \approx 7$, they effectively undergo back reactions in the radiolysis of pure water vapor so that the G value for stable end products from pure water vapor is very small as shown in Table 1.

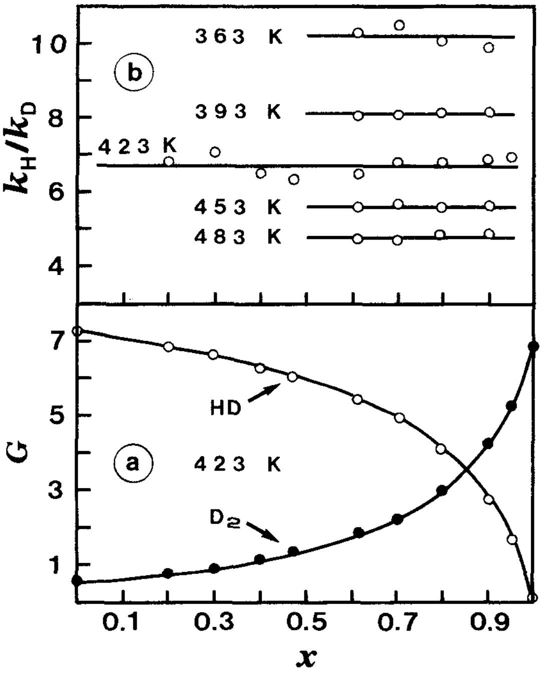

Fig. 1

a) The yields of HD and D_2 evolved in the gas-phase radiolysis of D_2O + ($c\text{-}C_6H_{12}$ + $c\text{-}C_6D_{12}$) mixtures as a function of x, where $x = [c\text{-}C_6D_{12}]/\{[c\text{-}C_6H_{12}] + [c\text{-}C_6D_{12}]\}$. $G(H_2)$, not shown, decreases with increasing x, and $G(H_2)_{x=0} = 0.13$. Dose = 5.0 kGy, p = 1.80 · 10^5 Pa, V = 0.54 dm^3, the total concentration of the additive = 0.50 mol%.

b) The kinetic isotope effects at various temperatures calculated from Eq. (16)

In Fig. 1a are shown as typical results the yields of isotopic hydrogen from D_2O vapor containing a small concentration of $c\text{-}C_6H_{12}$ + $c\text{-}C_6D_{12}$ mixtures. In the presence of low concentrations of RH + R′D, the $D^{\bullet}$ and $OD^{\bullet}$ radicals produced in reactions (3), (5), and (6) efficiently undergo abstraction of H and D atoms from the additives at temperatures higher than about 360 K:

$$\mathrm{D^{\bullet} + RH \xrightarrow{k_H} HD + R^{\bullet}} \tag{8}$$

$$\mathrm{D^{\bullet} + R'D \xrightarrow{k_D} D_2 + R'^{\bullet}} \tag{9}$$

$$\mathrm{OD^{\bullet} + RH \longrightarrow HDO + R^{\bullet}} \tag{10}$$

$$\mathrm{OD^{\bullet} + R'D \longrightarrow D_2O + R'^{\bullet}} \tag{11}$$

$$\mathrm{R^{\bullet} + R^{\bullet} \longrightarrow RH + R(-H)} \tag{12}$$

$$\mathrm{R^{\bullet} + R^{\bullet} \longrightarrow R-R.} \tag{13}$$

In the case where cyclohexane was taken as an additive, we have quantitatively determined not only isotopic hydrogen but also cyclohexene and bicyclohexyl yields [18], and the material balance confirmed the above scheme, i.e., $G(\mathrm{HD} + \mathrm{D_2}) = G(\text{cyclohexene}) + G(\text{bicyclohexyl})$.

3.2. Determination of the Kinetic Isotope Effect

It has been shown [13–16] that the yields of HD and D_2 in Fig. 1a can be represented by Eqs. (14) and (15), respectively,

$$G(\mathrm{HD}) = g(\mathrm{D^{\bullet}})\frac{k_H[\mathrm{RH}]}{k_H[\mathrm{RH}] + k_D[\mathrm{R'D}] + k_Y[\mathrm{Y}]} \tag{14}$$

$$G(\mathrm{D_2}) = g(\mathrm{D_2}) + g(\mathrm{D^{\bullet}})\frac{k_D[\mathrm{R'D}]}{k_H[\mathrm{RH}] + k_D[\mathrm{R'D}] + k_Y[\mathrm{Y}]} \tag{15}$$

where the measured yields are denoted by G, and the primary yields in water vapor by g. The $g(D_2)$ value is that for the unimolecularly detached deuterium. Combination of Eqs. (14) and (15) gives

$$\frac{k_H}{k_D} = \frac{G(\mathrm{HD})}{G(\mathrm{D_2}) - g(\mathrm{D_2})}\frac{[\mathrm{R'D}]}{[\mathrm{RH}]} = \frac{G(\mathrm{HD})}{G(\mathrm{D_2}) - g(\mathrm{D_2})}\frac{x}{1-x} \tag{16}$$

which permits the k_H/k_D value to be calculated as a function of x, where $x = [\mathrm{R'D}]/\{[\mathrm{RH}] + [\mathrm{R'D}]\}$.

Fig. 1b displays the isotope effects at different temperatures calculated from Eq. (16). As can be seen from Fig. 1b, the ratios k_H/k_D at a constant temperature are independent of the ratios $[\mathrm{R'D}]/[\mathrm{RH}]$ over a wide range, indicating the validity of Eq. (16). From the temperature dependence of the KIEs shown in Fig. 1b, the ratio A_H/A_D and the difference in activation energy $E_D - E_H$ were computed with the aid of a least-mean-squares fitting program. The results for the reactions of D-atoms with different alkanes are gathered in Table 2 along with the data previously determined for the reactions of hydrogen atoms with alkanes.

The radiolysis of heavy water vapor probably produces translationally hot deuterium atoms. However, the concentration of added hydrocarbon mixtures in heavy water vapor was such that $\{[\mathrm{RH}] + [\mathrm{R'D}]\} \ll [\mathrm{D_2O}]$. Hence, even if hot deuterium atoms are produced in the radiolysis of heavy water vapor, they should undergo many collisions with water molecules and should be thermalized before they react with the added hydrocarbons. Thus, the data in Table 2 are considered to reflect the KIEs for thermal hydrogen and deuterium atoms.

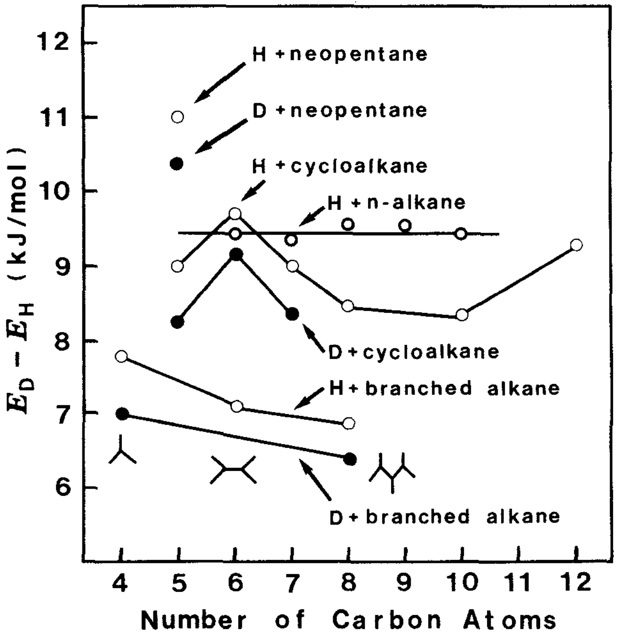

Fig. 2

The $E_D - E_H$ values for the reactions of H-atoms and D-atoms with the alkanes vs. the number of carbon atoms in the alkanes

4. Discussion

4.1. Molecular Structures and the $E_D - E_H$ Values

In order to reveal the relation between the $E_D - E_H$ values and the molecular structures, the values in Table 2 are plotted in Fig. 2 as a function of the number of carbon atoms

Table 2
Experimental kinetic isotope effects for abstraction of hydrogen and deuterium atoms from the alkanes by hydrogen and deuterium atoms

Reaction	k_H/k_D[a]		Temperature range (K)	Ref.
	A_H/A_D	$(E_D - E_H)$ kJ/mol		
$D + neo\text{-}C_5H_{12}/neo\text{-}C_5D_{12}$[b]	0.36 ± 0.04	10.38 ± 0.42	373−463	[c]
$D + c\text{-}C_5H_{10}/c\text{-}C_5D_{10}$	0.63 ± 0.06	8.24 ± 0.29	363−463	[c]
$D + c\text{-}C_6H_{12}/c\text{-}C_6D_{12}$	0.49 ± 0.04	9.16 ± 0.25	363−483	[c]
$D + c\text{-}C_7H_{14}/c\text{-}C_7D_{14}$	0.56 ± 0.03	8.37 ± 0.17	363−483	[c]
$D + n\text{-}C_7H_{16}/n\text{-}C_7D_{16}$	0.53 ± 0.06	8.79 ± 0.38	363−473	[c]
$D + i\text{-}C_4H_{10}/i\text{-}C_4D_{10}$	0.66 ± 0.06	7.03 ± 0.29	373−463	[c]
$D + (CH_3)_2CHCH(CH_3)CH(CH_3)_2/$ $(CD_3)_2CDCD(CD_3)CD(CD_3)_2$[d]	0.70 ± 0.15	6.44 ± 0.71	373−433	[c]
$H + neo\text{-}C_5H_{12}/neo\text{-}C_5D_{12}$	0.32 ± 0.04	11.00 ± 0.46	373−483	[15]
$H + c\text{-}C_5H_{10}/c\text{-}C_5D_{10}$	0.54 ± 0.04	9.00 ± 0.25	363−463	[15]
$H + c\text{-}C_6H_{12}/c\text{-}C_6D_{12}$	0.43 ± 0.03	9.67 ± 0.25	363−463	[14]
$H + c\text{-}C_7H_{14}/c\text{-}C_7D_{14}$	0.50 ± 0.04	9.00 ± 0.25	363−483	[15]
$H + c\text{-}C_8H_{16}/c\text{-}C_8D_{16}$	0.56 ± 0.03	8.45 ± 0.17	363−463	[15]
$H + c\text{-}C_{10}H_{20}/c\text{-}C_{10}D_{20}$	0.55 ± 0.05	8.41 ± 0.33	363−463	[15]
$H + c\text{-}C_{12}H_{24}/c\text{-}C_{12}D_{24}$	0.48 ± 0.05	9.29 ± 0.33	363−463	[15]
$H + n\text{-}C_6H_{14}/n\text{-}C_6D_{14}$	0.45 ± 0.04	9.46 ± 0.29	363−463	[14]
$H + n\text{-}C_7H_{16}/n\text{-}C_7D_{16}$	0.46 ± 0.05	9.37 ± 0.38	363−473	[14]
$H + n\text{-}C_8H_{18}/n\text{-}C_8D_{18}$	0.44 ± 0.06	9.58 ± 0.46	373−463	[14]
$H + n\text{-}C_9H_{20}/n\text{-}C_9D_{20}$	0.45 ± 0.03	9.54 ± 0.25	373−463	[14]
$H + n\text{-}C_{10}H_{22}/n\text{-}C_{10}D_{22}$	0.47 ± 0.03	9.41 ± 0.21	363−463	[14]
$H + i\text{-}C_4H_{10}/i\text{-}C_4D_{10}$	0.60 ± 0.11	7.78 ± 0.63	373−463	[15]
$H + (CH_3)_2CHCH(CH_3)_2/$ $(CD_3)_2CDCD(CD_3)_2$[e]	0.70 ± 0.08	7.07 ± 0.38	363−463	[15]
$H + (CH_3)_2CHCH(CH_3)CH(CH_3)_2/$ $(CD_3)_2CDCD(CD_3)CD(CD_3)_2$[d]	0.75 ± 0.05	6.82 ± 0.21	363−463	[15]
$H + CH_3C_6H_{11}/CD_3C_6D_{11}$[f]	0.51 ± 0.04	8.58 ± 0.25	363−483	[16]

[a] $k_H/k_D = A_H/A_D \exp((E_D - E_H)\,(\text{kJ mol}^{-1})/RT)$.

[b] Abbreviations of $D^{\bullet} + neo\text{-}C_5H_{12} \xrightarrow{k_H} HD + C_5H^{\bullet}_{11}$ and $D^{\bullet} + neo\text{-}C_5D_{12} \xrightarrow{k_D} D_2 + C_5D^{\bullet}_{11}$.

[c] This work.

[d] 2,3,4-Trimethylpentane.

[e] 2,3-Dimethylbutane.

[f] Methylcyclohexane.

in the alkanes. Some characteristic features of Fig. 2 are enumerated as follows:

(i) The $E_D - E_H$ value diminishes in going from neopentane through n-alkanes to isoalkanes.
(ii) The value of $E_D - E_H$ for the cycloalkanes varies with the increasing number of carbon atoms in a complicated fashion.
(iii) In contrast to the cycloalkanes, n-alkanes from n-hexane to n-decane exhibit fairly constant $E_D - E_H$ values, which are independent of the chain lengths.
(iv) The deuterium atom as an attacking species gives a slightly smaller $E_D - E_H$ value than the hydrogen atom. This is the case for all hydrocarbons studied.

Since detailed discussion of points (i)−(iii) was made in our previous paper [15], it suffices to give concise explications for (i)−(iii).

Point (i) is rationalized by invoking the Evans-Polanyi relation. The primary, secondary, and tertiary C−H bond energies in neopentane, n-alkane, and isobutane are known to decrease in this order. For these alkanes, the decrease in the C−H bond energy is accompanied by the concomitant decrease in the $E_D - E_H$ value. This indicates that the magnitude of the $E_D - E_H$ values is governed by the strength of the C−H bond being broken. For the reaction of a reactive species with a homologous series of compounds, Evans and Polanyi [19], suggested a linear relationship between the activation energy E and the enthalpy change of the reaction, ΔH_r. For the attack of deuterium atoms on C−H bonds in a homologous series of the alkanes, the enthalpy change can be replaced by the bond energy $D(C-H)$ of the C−H bond involved [20]

$$E_H = a_H[D(C-H)] + b_H \tag{17}$$

where a_H and b_H are constants. Likewise, for the attack of deuterium atoms on C−D bonds in the corresponding perdeuterated alkanes, it follows that

$$E_D = a_D[D(C-D)] + b_D\,. \tag{18}$$

Subtracting Eq. (17) from Eq. (18) leads to

$$E_D - E_H = a_D[D(C-D)] - a_H[D(C-H] + b_D - b_H\,. \tag{19}$$

The difference in the bond energies between C−H and C−D bonds is not well-known for a given alkane. However, with the assumption that $D(C-D) - D(C-H) = \text{constant}$ for a family of closely related alkanes, we arrive at the pseudo-Evans-Polanyi equation

$$E_D - E_H = a[D(C-H)] + b \tag{20}$$

where $a = a_D - a_H$ and $b = b_D - b_H +$ (constant) a_D. Then, a linear relation between $E_D - E_H$ and D(C−H) is anticipated to exist unless $a_D = a_H$. In Fig. 3 the values of $E_D - E_H$ for the reaction of D-atoms with the alkanes are plotted vs. the known C−H bond strengths of neo-C_5H_{11}−H [21], c-C_5H_9−H [22], c-C_6H_{11}−H [22], and t-C_4H_9−H [21]. Fig. 3 includes the $E_D - E_H$ values for the reaction of H-atoms with the paraffins [15]. Fig. 3 shows that the quasi-Evans-Polanyi relation, Eq. (20), is applicable to the reactions of both H-atoms and D-atoms with various alkanes.

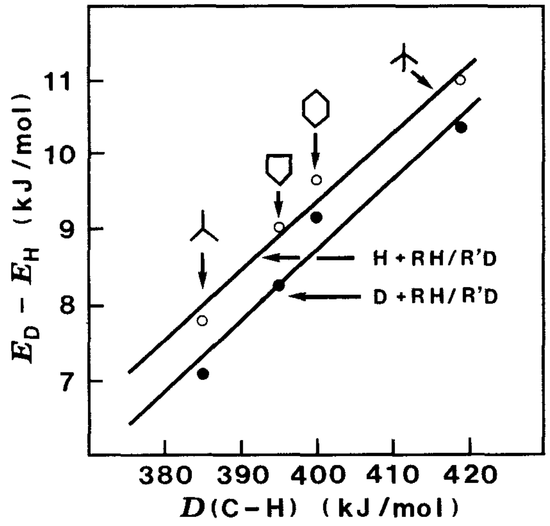

Fig. 3
The linear relationships between the $E_D - E_H$ values and the C−H bond energies of the alkanes

It should be noted in this context that the $E_D - E_H$ values for isobutane are taken to represent the difference in the activation energies for abstraction from the tertiary C−D and C−H bonds in isobutanes. This seems to be justified because when accepting the recommended rate constants for H-abstraction from the primary and tertiary C−H bonds in the alkanes by H-atoms [5], one can conclude that the contribution from the tertiary C−H bond to the total rate of H-abstraction from isobutane amounts to about 93% at the midpoint of the temperature range covered in the present study, 423 K.

We now address ourselves to point (ii). As emphasized in the preceding argument, the $E_D - E_H$ values are largely governed by the strength of breaking C−H bonds. Then the irregular change in the $E_D - E_H$ value for the cycloparaffins shown in Fig. 2 should be associated with the variation of the C−H bond energies for the cyclanes. Unfortunately, the C−H bond energy is not available for the large ring size compounds. There is, however, a clue to deducing it. It has been recognized by several investigators [23, 24] that the ring strain has marked effects on reaction rates. Brown [23], for instance, proposed the Internal strain (I-strain) hypothesis from systematic studies of the effects of the ring strain on the solvolysis rate. In this hypothesis, the difference in strain energy between the reactant and the transition state is conjectured to have a strong influence on the magnitude of the Arrhenius activation energy. When applied to our problem, the I-strain hypothesis can be expressed [25] in the form

$$D(\text{cycloalkane C}-\text{H}) = D(\text{standard secondary C}-\text{H}) + [E_S(\text{cycloalkene}) - E_S(\text{cycloalkane})]/2 \qquad (21)$$

where E_S stands for the conventional strain energy. In utilizing Eq. (21), a secondary C−H bond energy in strain-free n-butane [22] is adopted as D(standard secondary C−H). The estimated C−H bond energies are summarized in Table 3 and are plotted in Fig. 4. A comparison of Figs. 2 and 4 discloses that the $E_D - E_H$ values for the cyclanes run parallel to the estimated C−H bond energies.

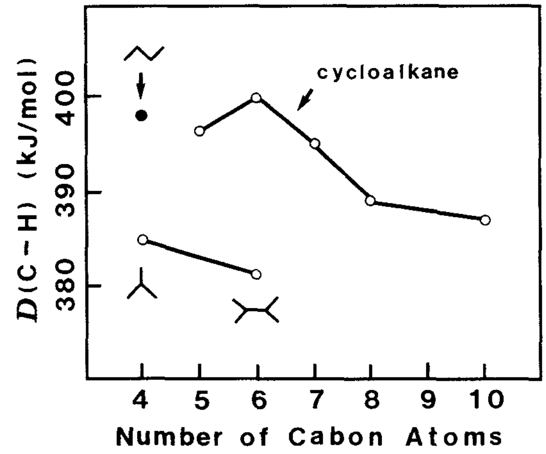

Fig. 4
The estimated C−H bond energies for the cycloalkanes and branched alkanes vs. the number of carbon atoms in the alkanes

The unknown tertiary C−H bond energies in 2,3-dimethylbutane (2,3-DMB) and 2,3,4-trimethylpentane (2,3,4-TMP) should, in principle, be inferable from an equation similar to Eq. (21), viz.,

$$D(\text{tertiary C}-\text{H}) = D(\text{standard tertiary C}-\text{H}) + [E_S(\text{alkene}) - E_S(\text{alkane})]/2\,. \qquad (22)$$

The bond strength of the tertiary C−H bond in 2,3-DMB was calculated by taking the tertiary C−H bond energy in strain-free isobutane as D(standard tertiary C−H). The result is listed in Table 3 and shown in Fig. 4. Eq. (22) indicates that the tertiary C−H bond is appreciably weaker in 2,3-DMB than in isobutane in good accord with the experimental finding.

Point (iii) is interpreted to imply that abstraction of a hydrogen atom takes place mainly from the secondary C−H bonds and that the average bond energy of the secondary C−H bonds barely depends on the chain lengths of the n-alkanes studied.

We now turn our attention to point (iv). The pronounced difference in reactivity between C−H and C−D bonds can be qualitatively ascribed to the difference in zero-point energy (E_0) for C−H and C−D bonds. However, the slight reactivity difference between H-atoms and D-atoms as the attacking species cannot be accounted for in any qualitative manner. In this regard, the theoretical approach would be helpful as described in detail in the next section.

Table 3
C−H bond dissociation energies

Compound	Strain energy[a] (kJ mol^{-1})		C−H bond energy[a] (kJ mol^{-1})	
	Alkene	Alkane	Exptl.	Eq. (21)
c-C_5H_{10}	23.8	25.9	394.1	396.5
c-C_6H_{12}	5.4	0.0	399.6	400.2
c-C_7H_{14}	21.3	25.9	387.0	395.2
c-C_8H_{16}	24.3	40.2	–	389.6
c-$C_{10}H_{20}$	29.3	51.5	–	386.4
c-$C_{12}H_{24}$	–	16.7	–	–
n-C_4H_{10}	0.0	0.0	397.5	397.5
i-C_4H_{10}	0.0	0.0	384.9	384.9[b]
2,3-DMB[c]	4.6	11.3[d]	–	381.6[b]
2,3,4-TMP[e]	–	16.4	–	–

[a] Ref. [15].
[b] Calculated from Eq. (22).
[c] 2,3-Dimethylbutane.
[d] C. Rüchardt and H.-B. Beckhaus, Angew. Chem. Int. Ed. Engl. *19*, 429 (1980).
[e] 2,3,4-Trimethylpentane.

4.2. Theoretical Calculation of the Kinetic Isotope Effects

One of the merits of transition-state theory lies in its ability of allowing quantitative predictions of the primary KIE. We have already achieved the theoretical estimation of the KIEs for the reactions of hydrogen atoms with some alkanes [14,15] within the framework of transition-state theory [26a−29] and have found good agreement between experiment and theory. In the present work, an attempt is made to extend the theoretical calculations to the reaction of deuterium atoms with several alkanes. Neopentane, cyclohexane, and isobutane are chosen among others for the theoretical calculations as prototype alkanes possessing the primary, secondary, and tertiary C−H bonds.

To perform the theoretical calculation of the KIE based on transition-state theory, all vibrational frequencies of the reactants and activated complexes have to be known in principle. Although during the past decade considerable progress has been made in ab initio calculation of the vibrational frequencies for neutral molecules [30], radical species [31], and activated complexes [32], the quantum mechanical approach seems difficult to apply to our problem. Hence we employ a simplified collinear three-atom model written by

$$A + BC \longrightarrow [A{-}{-}{-}B{-}{-}{-}C]^{\ddagger} \longrightarrow AB + C \qquad (23)$$

where A refers to the attacking atom, B is the atom transferred in the reaction (H or D), and C is the residual group. The theoretical formula of the KIE for the aligned three-atom model is of the form [26a−28]

$$\frac{k_H}{k_D} = \frac{\nu_{iH}}{\nu_{iD}}\left(\frac{\Gamma_H}{\Gamma_D}\right)^{*}\left(\frac{\Gamma_{sH}\Gamma_{bH}^2}{\Gamma_{sD}\Gamma_{bD}^2}\right)^{\ddagger}\left(\frac{\Gamma_{sD}}{\Gamma_{sH}}\right)^{r}. \qquad (24)$$

In this equation, ν_i is the imaginary frequency corresponding to motion along the reaction coordinate, Γ^* represents the tunnel correction factor, $\Gamma^{\ddagger}$ and Γ^r denote quantum correction factors for each of the real vibrations of the activated complex and the reactant and take the form $\Gamma = (u/2)/\sinh(u/2)$ with $u = h\nu/kT$, and subscripts s and b refer to the stretching and bending modes of vibrations.

Table 4
Molecular properties of neo-$C_5H_{11}-H$, c-$C_6H_{11}-H$, tert-C_4H_9-H, and H−H

Property	neo-$C_5H_{11}-H$[a]	c-$C_6H_{11}-H$[a]	tert-C_4H_9-H	H−H[a]
D_{298}^0 (kJ mol^{-1})	419.66	399.57	390.2[b]	431.56
$\tilde{\nu}_s$ (cm^{-1})	2959[c] (2218)	2933[c] (2206)	2880[c] (2067)	4395.2
D_e (kJ mol^{-1})[d]	437.36	417.1	407.43	457.86
r_0 (Å)[e]	1.114	1.119	1.122	0.7417
β (Å^{-1})[f]	1.817	1.844	1.832	1.9420
ζ[g]	0.10	0.10	0.10	0.10

[a] Ref. [15].
[b] R. R. Baldwin, G. R. Drewery, and R. W. Walker, J. Chem. Soc., Faraday Trans. I *80*, 2827 (1984).
[c] C−H stretching frequency: C−D stretching frequency is in parenthesis.
[d] $D_e = D_{298}^0 + E_0$*).
[e] Equilibrium bond length.
[f] Morse parameter.
[g] Sato parameter.

Table 5
Some properties of the activated complexes calculated by using the aligned three-atom model $A + BC \rightarrow AB + C$[a]

Property	H--H--neo-C_5H_{11}[b]	H--H--c-C_6H_{11}[b]	H--H--tert-C_4H_9
$V^{\ddagger}$ (kJ mol^{-1})	49.231	38.014	34.333
$r_{AB}^{\ddagger}$ (Å)	0.9968	1.0479	1.0762
$r_{BC}^{\ddagger}$ (Å)	1.2916	1.2563	1.2455
$F_{AB}^{\ddagger}$ (mdyn/Å)	0.306	0.081	0.000
$F_{BC}^{\ddagger}$ (mdyn/Å)	0.981	1.433	1.597
$F_{AC}^{\ddagger}$ (mdyn/Å)	1.640	1.492	1.395
$F_{\theta}^{\ddagger}$ (10^{11} erg/rad^2)	0.081	0.073	0.070

[a] Calculated from the LEPS potential-energy surface with $\zeta = 0.10$.
[b] Ref. [15].

Table 6
Vibrational frequencies of the activated complexes[a]

Activated complex	Vibrational frequency (cm^{-1})			E_0 (activated complex) (kJ mol^{-1})
	$\tilde{\nu}_s$	$\tilde{\nu}_b$[b]	$\tilde{\nu}_i$[c]	
H--H--neo-C_5H_{11}	1329	756	2113i	17.00
H--D--neo-C_5D_{11}	1268	598	1622i	14.74
D--H--neo-C_5H_{11}	1027	709	2003i	14.63
D--D--neo-C_5D_{11}	996	538	1508i	12.40
H--H--c-C_6H_{11}	1334	704	1978i	16.41
H--D--c-C_6D_{11}	1239	554	1560i	14.04
D--H--c-C_6H_{11}	1060	662	1823i	14.26
D--D--c-C_6D_{11}	1005	501	1405i	12.01
H--H--t-C_4H_9	1340	678	1891i	16.13
H--D--t-C_4D_9	1228	532	1512i	13.71
D--H--t-C_4H_9	1081	639	1717i	14.11
D--D--t-C_4D_9	1011	482	1341i	11.82

[a] Calculated from the properties of the activated complexes shown in Table 5.
[b] Doubly degenerate.
[c] Imaginary frequency.

---

*) E_0 = Zero point-Energy.

First of all, the potential-energy surface is constructed by using the semiempirical London-Eyring-Polanyi-Sato (LEPS) formula [33] with a single adjustable parameter. Table 4 lists the selected molecular constants as input data to the LEPS calculation. As an example, the potential-energy surface near the saddle point is displayed in Fig. 5 for the reaction of a hydrogen atom with cyclohexane. Incorporated in Fig. 5 are orthogonal coordinates ϱ and σ, of which ϱ designates the reaction coordinate and σ is perpendicular to ϱ. Within the Born-Oppenheimer approximation, the same potential-energy surface as Fig. 5 holds in the reaction of a deuterium atom with cyclohexane as well.

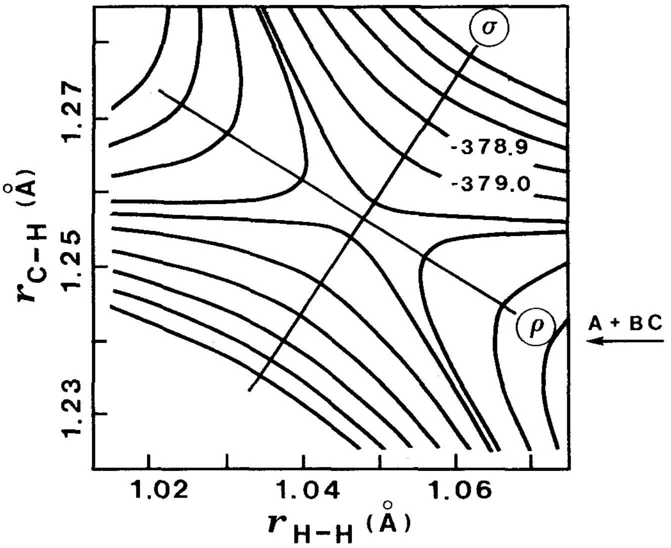

Fig. 5
Potential-energy surface calculated from the LEPS equation for the collinear reaction $H^{\bullet} + c\text{-}C_6H_{12} \rightarrow H_2 + c\text{-}C_6H_{11}^{\bullet}$. Included are the orthogonal coordinates ϱ and σ, of which ϱ is the reaction coordinate. Energy units = (kJ/mol)

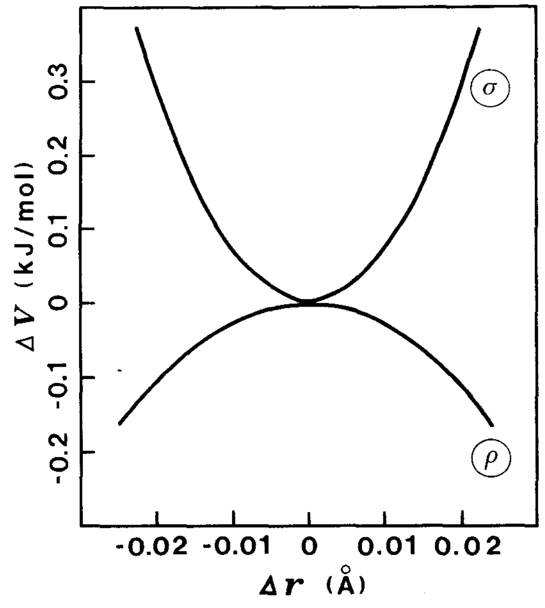

Fig. 6
LEPS potential-energy profiles along the coordinates ϱ and σ

Fig. 6 shows the potential-energy profiles along the axes ϱ and σ. For small departures from the saddlepoint, the potential-energy profiles can be adequately approximated by the quadratic expression, $\Delta V = \frac{1}{2} F(\Delta r)^2$, where F is the force constant. When one depicts the potential profiles over an extended region about the saddlepoint, the anharmonicity becomes discernible, and the profiles can no longer be fitted to the quadratic form. Table 5 contains the force constants for the activated complexes evaluated from the standard analysis [26b] of the LEPS surfaces. These force constants enable us to derive the vibrational frequencies for the twelve different activated complexes as compiled in Table 6.

Finally we are faced with the tunnel correction factor Γ^*. The term Γ^*, expressing the nuclear tunneling by the light atom (H or D), is given by [26c]

$$\Gamma^* = \frac{\exp(V_1/RT)}{RT} \cdot \int_0^\infty \left\{1 - \frac{\cosh 2\pi(a-b) + \cosh 2\pi d}{\cosh 2\pi(a+b) + \cosh 2\pi d}\right\} \exp(-E/RT)\,\mathrm{d}E \qquad (25)$$

where a, b, and d are functions of the imaginary frequency ν_i, potential-barrier heights V_1 and V_2, temperature T and energy E of the system, and are defined elsewhere [26c]. Eq. (25) is integrated numerically by a computer using the Romberg method. Throughout the tunnel calculations, the tunnel barrier heights V_1 and V_2 are taken to be

$$V_1 = V^{\ddagger} + E_0(\text{activated complex}) - E_0(\text{reactant})$$

$$V_2 = V^{\ddagger} + E_0(\text{activated complex}) - E_0(\text{product}) + \Delta D_e$$

where $\Delta D_e = D_e(\text{product}) - D_e(\text{reactant})$ and the values for D_e can be found in Table 4. More detailed procedures of the tunnel calculations were described in our previous work [14, 16]. Recent methods [34, 35] for making the tunnel corrections seem to be more sophisticated than that used in the present calculations.

Table 7
Experimental and theoretical kinetic isotope effects

T (K)	$(k_H/k_D)_{exptl}$	$(k_H/k_D)_{calcd}$	$(k_H/k_D)_{exptl}$	$(k_H/k_D)_{calcd}$
	$H + neo\text{-}C_5H_{12}/neo\text{-}C_5D_{12}$		$D + neo\text{-}C_5H_{12}/neo\text{-}C_5D_{12}$	
373	11.11	11.70	10.22	11.45
423	7.30	7.51	6.88	7.46
473	5.25	5.47	5.04	5.48
	$H + c\text{-}C_6H_{12}/c\text{-}C_6D_{12}$		$D + c\text{-}C_6H_{12}/c\text{-}C_6D_{12}$	
373	9.72	8.62	9.41	7.39
423	6.72	5.87	6.63	5.39
473	5.03	4.46	5.04	4.26
	$H + iso\text{-}C_4H_{10}/iso\text{-}C_4D_{10}$		$D + iso\text{-}C_4H_{10}/iso\text{-}C_4D_{10}$	
373	7.37	6.84	6.37	6.92
423	5.48	5.10	4.87	5.16
473	4.34	4.08	3.94	4.15

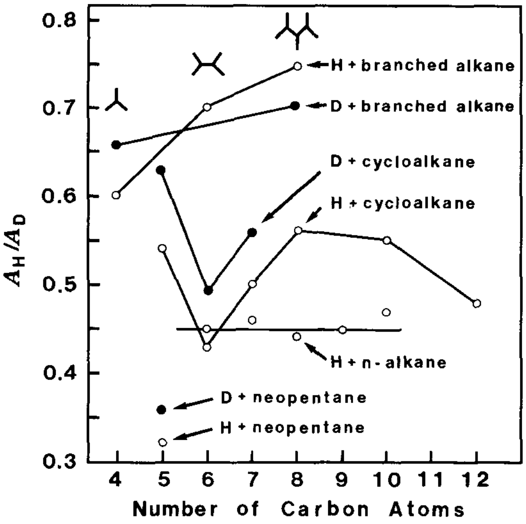

Fig. 7
Ratios A_H/A_D vs. the number of carbon atoms in the alkanes

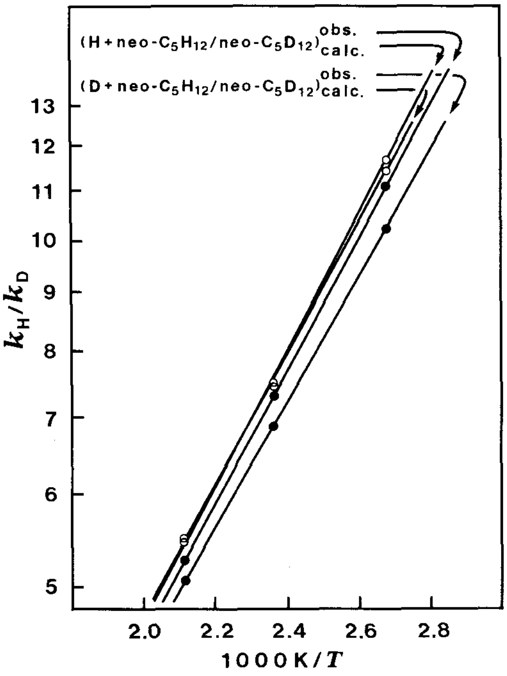

Fig. 8
Comparison between the experimental and theoretical KIEs for the reactions $H^{\bullet}$ + neo-C_5H_{12}/neo-C_5D_{12} and $D^{\bullet}$ + neo-C_5H_{12}/neo-C_5D_{12}

Qualitatively speaking, the importance of the tunnel effect manifests itself in an abnormally low ratio A_H/A_D. A ratio A_H/A_D smaller than one half is taken as strong evidence for the occurrence of the tunnel phenomenon [36]. Many of the ratios A_H/A_D assembled in Table 2 are less than $\frac{1}{2}$ or nearly equal to $\frac{1}{2}$, and satisfy the above criterion. Fig. 7 illustrates the variation in the ratios A_H/A_D with the molecular structures. The A_H/A_D values are mirror images of the $E_D - E_H$ values shown in Fig. 2. That is, the larger the $E_D - E_H$ value the smaller the ratio A_H/A_D becomes. This trend lends support to the view that tunneling is operating in our system, since the tunneling tends to make the value for $E_D - E_H$ greater and the ratio A_H/A_D smaller [36].

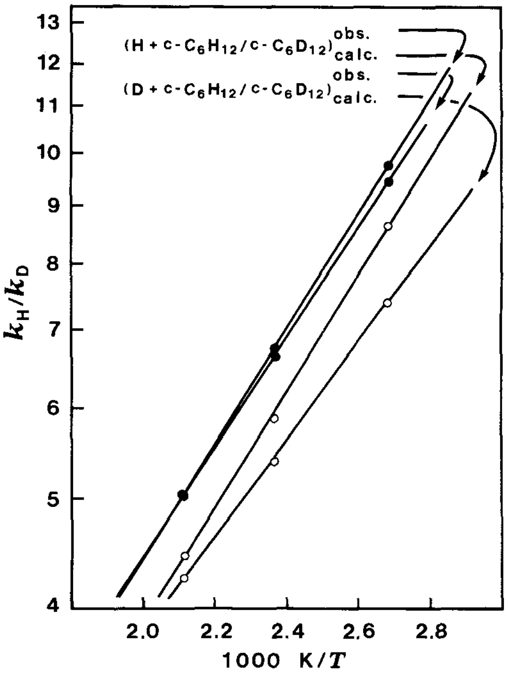

Fig. 9
Experimental and theoretical KIEs for the reactions $H^{\bullet}$ + c-C_6H_{12}/c-C_6D_{12} and $D^{\bullet}$ + c-C_6H_{12}/c-C_6D_{12}

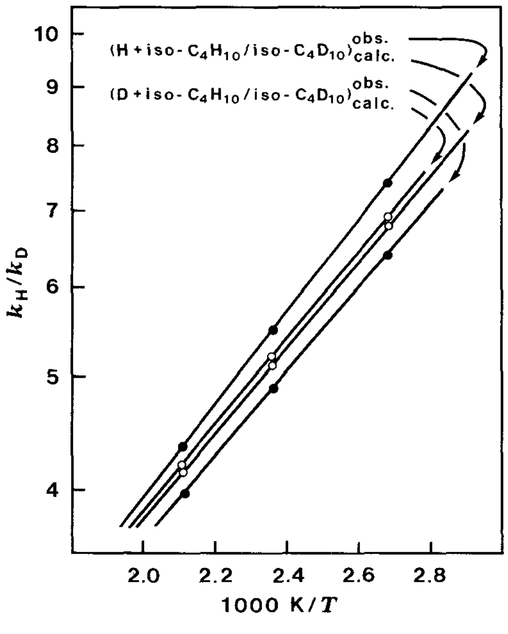

Fig. 10
Experimental and theoretical KIEs for the reactions $H^{\bullet}$ + iso-C_4H_{10}/iso-C_4D_{10} and $D^{\bullet}$ + iso-C_4H_{10}/iso-C_4D_{10}

Having computed all terms appearing in Eq. (24), we are now in a position to compare the calculated KIEs listed in Table 7 with experimental data. Figs. 8–10 make comparisons between experiment and theory. Generally speaking, the agreement between experiment and theory is gratifying in view of the fact that the KIEs for the six reactions were calculated without changing the Sato parameter from one reaction to the next. However, some qualitative discrepancies between experiment and theory will be found by close inspection of Figs. 8–10. Our experimental KIEs for the reactions, H$^\bullet$ + RH/R′D, are larger, albeit slightly, than those for the reactions, D$^\bullet$ + RH/R′D, irrespective of the pair of RH/R′D. The theoretical calculation could reproduce this tendency only for the abstraction reaction from cyclohexane (Fig. 9). With neopentane and isobutane (Figs. 8, 10), the theoretical KIEs for H$^\bullet$ + RH/R′D are essentially the same magnitude as those for D$^\bullet$ + RH/R′D. In spite of these small failings, the theoretical calculations based on transition-state theory and the simplified three atom model are capable of reproducing the major features of the experimental KIEs.

In our previous work [13], the Bond-Energy-Bond-Order method [26] was used in place of the LEPS method to calculate the properties of the activated complex for the reaction of a hydrogen atom with cyclohexane. Even though tunnel correction factors were taken into consideration in that work, the calculated KIEs were much smaller than the experimental ones. Thus, it seems necessary to incorporate the tunnel effect in order to match our experimental KIEs with theoretical values, irrespective of the method of calculating the potential-energy surface.

The authors wish to thank Mrs. M. Goël for experimental assistance. They are also indebted to the Swiss National Science Foundation for a grant.

References

[1] J. R. McNesby and H. Okabe, in: "Advances in Photochemistry", Vol. 3, pp. 157–240, eds. W. A. Noyes, Jr., G. S. Hammond, and J. N. Pitts, Jr., Interscience, New York 1964.
[2] P. Ausloos and S. G. Lias, in: "Chemical Spectroscopy and Photochemistry in the Vacuum-Ultraviolet", pp. 465–482, eds. C. Sandorfy, P. J. Ausloos, and M. B. Robin, Reidel, Dordrecht, Holland 1974.
[3] N. Fujisaki and T. Gäumann, Radiat. Phys. Chem. *23*, 49 (1984).
[4] I. György, in: "Radiation Chemistry of Hydrocarbons", pp. 61–175, ed. G. Földiák, Elsevier, Amsterdam 1981.
[5] R. R. Baldwin and R. W. Walker, J. Chem. Soc., Faraday Trans. I *75*, 140 (1979).
[6] R. M. Marshall, H. Purnell, and A. Sheppard, J. Chem. Soc., Faraday Trans. I *80*, 2999 (1984).
[7] J. N. Bradley and K. O. West, J. Chem. Soc., Faraday Trans. I *72*, 8 (1976).
[8] J.-R. Cao and M. H. Back, Can. J. Chem. *62*, 86 (1984).
[9] K. Hoyermann, A. W. Preuss, and H. Gg. Wagner, Ber. Bunsenges. Phys. Chem. *79*, 156 (1975).
[10] D. Mihelcic, V. Schubert, F. Höfler, and P. Potzinger, Ber. Bunsenges. Phys. Chem. *79*, 1230 (1975).
[11] W. E. Jones, S. D. MacKnight, and L. Teng, Chem. Rev. *73*, 407 (1973).
[12] J. A. Kerr and S. J. Moss, "Handbook of Bimolecular and Termolecular Gas Reactions", Vol. I, pp. 9–61, CRC Press, Boca Raton, Florida 1981.
[13] N. Fujisaki and T. Gäumann, Ber. Bunsenges. Phys. Chem. *81*, 544 (1977).
[14] N. Fujisaki, A. Ruf, and T. Gäumann, J. Chem. Phys. *80*, 2570 (1984).
[15] N. Fujisaki, A. Ruf, and T. Gäumann, J. Am. Chem. Soc. *107*, 1605 (1985).
[16] N. Fujisaki, A. Ruf, and T. Gäumann, Helv. Chim. Acta *68*, 1168 (1985).
[17] T. Gäumann, O. Piringer, and A. Weber, Chimia *24*, 112 (1970).
[18] N. Fujisaki and T. Gäumann, Int. J. Chem. Kinet. *14*, 1059 (1982).
[19] M. G. Evans and M. Polanyi, Trans. Faraday Soc. *34*, 11 (1938).
[20] J. A. Kerr, Chem. Rev. *66*, 465 (1966).
[21] J. A. Kerr, in: "Handbook of Chemistry and Physics", 65th ed., p. F-182, ed. R. C. Weast, CRC Press, Boca Raton, Florida 1984–1985.
[22] K. C. Ferguson and E. Whittle, Trans. Faraday Soc. *67*, 2618 (1971).
[23] H. C. Brown and M. Borkowski, J. Am. Chem. Soc. *74*, 1894 (1952).
[24] R. Heck and V. Prelog, Helv. Chim. Acta *38*, 1541 (1955).
[25] S. E. Stein and B. S. Rabinovitch, J. Phys. Chem. *79*, 191 (1975).
[26] H. S. Johnston, "Gas Phase Reaction Rate Theory", Ronald Press, New York 1966, (a) Chapter 13, (b) p. 333, (c) Chapter 2.
[27] J. Bigeleisen and M. Wolfsberg, in: "Advances in Chemical Physics", Vol. I, pp. 15–76, ed. I. Prigogine, Interscience, New York 1958.
[28] L. Melander and W. H. Saunders, Jr., "Reaction Rates of Isotopic Molecules", Wiley-Interscience, New York 1980.
[29] S. Glasstone, K. J. Laidler, and H. Eyring, "The Theory of Rate Processes", McGraw-Hill, New York 1941.
[30] See for example, (a) K. B. Wiberg, D. C. Dempsey, and J. J. Wendoloski, J. Phys. Chem. *88*, 5596 (1984); (b) P. Pulay, G. Fogarasi, G. Pongor, J. E. Boggs, and A. Vargha, J. Am. Chem. Soc. *105*, 7037 (1983).
[31] See for example, (a) J. Pacansky and B. Schrader, J. Chem. Phys. *78*, 1033 (1983); (b) M. N. Paddon-Row and J. A. Pople, J. Phys. Chem. *89*, 2768 (1985).
[32] See for example, (a) S. B. Brown, M. J. S. Dewar, G. P. Ford, D. J. Nelson, H. S. Rzepa, J. Am. Chem. Soc. *100*, 7832 (1978): (b) G. C. Schatz, A. F. Wagner, and T. H. Dunning, Jr., J. Phys. Chem. *88*, 221 (1984).
[33] (a) S. Sato, J. Chem. Phys. *23*, 592, 2465 (1955); (b) R. E. Weston, Jr., J. Chem. Phys. *31*, 892 (1959).
[34] R. A. Marcus and M. E. Coltrin, J. Chem. Phys. *67*, 2609 (1977).
[35] D. G. Truhlar and A. Kuppermann, J. Am. Chem. Soc. *93*, 1840 (1971).
[36] R. P. Bell, "The Tunnel Effect in Chemistry", Chapman and Hall, London 1980.

(Eingegangen am 1. November 1985, endgültige Fassung am 23. Dezember 1985) E 6122